SOBEL EDGE DETECTION AND ITS APPLICATION IN LMD-BASED SEISMIC FAULT DETECTION

KAI BAI[1], HUIQUN XU[2,3] and XIAOYU SHE[3]

[1] *School of Computer Science, Yangtze University, Jingzhou 434023, Hubei, P.R. China.*
[2] *Working Station for Postdoctoral Scientific Research, PetroChina Dagang Oilfield Company, Tianjin 300280, P.R. China.*
[3] *School of Geophysics and Oil Resources, Yangtze University, Wuhan 430100, Hubei, P.R. China.*

(Received January 12, 2018; revised version accepted September 30, 2018)

ABSTRACT

Bai, K., Xu, H.Q. and She, X.Y., 2018. Sobel edge detection and its application in LMD-based seismic fault detection. *Journal of Seismic Exploration*, 27: 531-542.

This paper aims to find a comprehensive method for detecting edges amidst background and noise. To this end, the local mean decomposition (LMD) filter and coherence algorithm were combined into a new seismic fault detection method. The priori knowledge on the edge location was calculated by the coherence cube, and the artificial edges were eliminated by the LMD filter. Then, the Sobel algorithm was adopted to obtain the greyscales based on the coherence, and derive the seismic edges. Through comparison, it is learned that the seismic edges obtained by our method coincide with the seismic faults in the original seismic data. Therefore, the proposed method can visualize seismic faults and accelerate the interpretation process. The research findings shed new light on the edge detection in relevant fields.

KEY WORDS: local mean decomposition (LMD), Sobel, edge detection, seismic fault detection.

INTRODUCTION

Edge detection is an important technique of image processing that localizes the major variations in greyscale image, and identifies their physical causes. The detection effect relies on how efficiently a process could detect near-edge intensity changes. The term “edge” may be defined as a set of connected pixels that forms a boundary between two disjoint regions (Rashmi et al., 2013). It has a great potential of application in 3D reconstruction, motion recognition, enhancement, restoration, registration and compression of images (Bahorich and Farmer, 1995; Ziou et al., 1998).

0963-0651/18/$5.00 © 2018 Geophysical Press Ltd.

Much research has been done on the application of edge detection in image processing. For instance, Cai et al. (2004) created a composite edge detector based on multiwavelet operator in the image. Nadernejad et al. (2008) compared the effect of several edge detection techniques in image processing. The existing edge detection algorithms for image analysis mainly concentrate on edge enhancement and edge detection (Nadernejad et al., 2008). Inspired by previous edge detection algorithms, Amstutz and Fehrenbach (2015) conducted a scale-space analysis and topological asymptotic analysis on edge detection.

The idea of edge detection has been adopted for identifying seismic faults, and the resultant "seismic edge detection" has been confirmed effective and feasible (Bahorich and Farmer, 1995; Luo et al., 1996; Carter and Lines, 2001). With the advent of image pre-processing algorithms, more mathematical algorithms have been introduced to enhance the edges in seismic images. By these algorithms, the seismic data are pre-processed through multiple steps to ensure the sound performance of seismic edge detection. Below are some typical algorithms for edge enhancement in fault detection. Focusing on image discontinuities, Di and Gao (2014) presented a greyscale transformation and an improved Canny edge detector for fault detection. Chehrazi et al. (2013) developed a cascaded workflow that enhances fault detection through attribute selection via the neural network. Phillips and Fomel (2017) proposed a plane-wave Sobel attribute for discontinuity enhancement, aiming to map the faults in seismic images. Wang et al. (2010) put forward a structure-oriented Gaussian (SOG) filter to reduce the noise in 3D reflection seismic data without sacrificing such details as structural and stratigraphic discontinuities and lateral heterogeneity. It should also be noted that edge detection techniques are highly sensitive to noise levels (Krešić-Jurić, 2012). Therefore, it would be difficult to differentiate the edges from the background and noise if an image is corrupted in multiple ways.

In light of the above, this paper proposes a new seismic fault detection method by processing seismic data with local mean decomposition (LMD) filter. The seismic filtering mechanism of the filter was explained to clarify its role in distinguishing the edges from the background and noise. Based on edge localization properties, the edges were sharpened by coherence such that the background was removed from the seismic data. After that, the author discussed the error of edge localization caused by noise. It is concluded that the robustness of seismic edge detection algorithms hinges on seismic data filtering and a priori knowledge of the coherence cube on seismic images.

LMD ADAPTIVE FILTER

Cohen (2002) laid down the fundamental ideas and methods of joint time-frequency distributions. As its name suggests, the theory depicts the energy or intensity of a signal simultaneously in time and frequency, and inspires the creation of the LMD for analysing nonlinear and nonstationary time series. The smoothed local mean of the LMD outperforms the cubic spline interpolation of empirical mode decomposition (EMD) in the extraction of amplitude- and frequency-modulated components (Park et al., 2011). The LMD was also adopted to decompose amplitude- and frequency-modulated signals into a small set of product functions, each of which is the product of an envelope signal and a frequency modulated signal, making it possible to derive a time-varying instantaneous phase and instantaneous frequency (Smith, 2005). The moving average filter is introduced to smooth the signal progressively for the LMD of a signal.

Specifically, the local magnitude function is determined by interpolating the absolute value of differences between successive extrema, and smoothing the signal using a moving average filter. The local mean is subtracted from the original signal, and then divided by the local magnitude function, seeking to obtain the frequency-modulated signal. Next, the mean values of successive extrema are interpolated by piecewise constant interpolation, and the moving average filter is adopted to output the local intrinsic mode function (IMF) and product function (PF). The LMD-based adaptive filter can be expressed as:

$$\hat{x}(t) = \sum PF_i(t) \quad , \tag{1}$$

where $\hat{x}(t)$ is an approximation of the target signal $x(t)$ (length: 2 sec). The signal can be reconstructed by eq. (1). As shown in Figs. 1 and 2, the IMF and PF components decomposed by LMD and EMD are arranged in descending order of frequency. It is possible to obtain a high-pass filter by removing low-frequency PF components and adding up the remaining ones. Similarly, a low-pass filter can be obtained by removing high-frequency PF components and adding up the remaining ones, and a bandpass filter can be derived by retaining only the PF components of medium frequency.

The Fourier transform spectrum of the target signal $x(t)$ obtained by the LMD is the same with that obtained by the EMD (Figs. 1a and 2a). It is the determination of local mean function that differentiates the LMD from the EMD concerning the same target signal $x(t)$. The LMD frequency components (Fig. 1b) are more intense than their EMD counterparts (Fig.2b) at 50 Hz. In particular, the highest-order component of PF is less intense than that of IMF (Figs. 1c, 1d, 1e and 1f; Figs. 2c, 2d, 2e and 2f) in the low frequency band. In addition, the LMD-based signal reconstruction has less residual error than the EMD-based procedure, as residual error exists not in Fig. 3a but in Fig. 3b. The above analysis proves the feasibility of a LMD-based filter in the frequency domain.

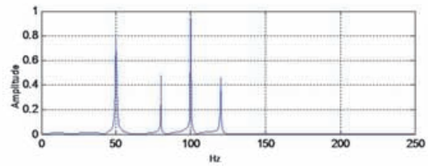

a) The frequency of the target signal $x(t)$

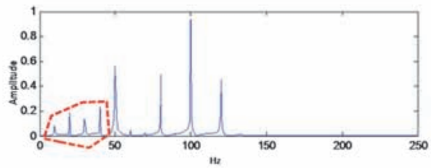

b) Order-1product function (PF1)

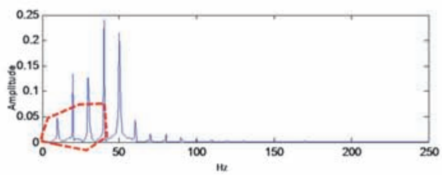

c) Order-2 product function (PF2)

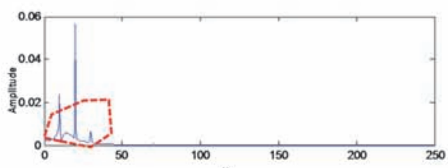

d) Order-3 product function (PF3)

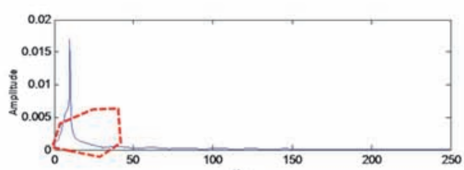

e) Order-4 product function (PF4)

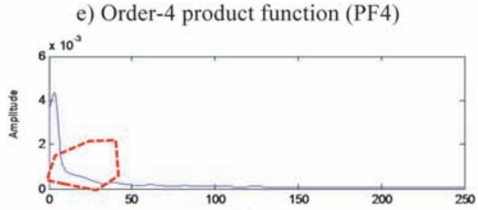

f) Order-5 product function (PF5)

Fig. 1. The PF components of the target signal obtained by the LMD.

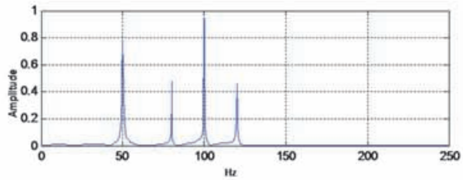

a) The frequency of the target signal $x(t)$

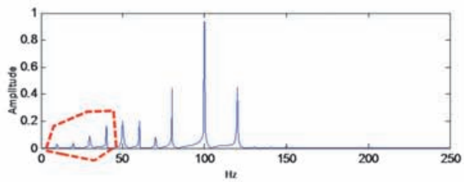

b) Order-1 intrinsic mode function (IMF1)

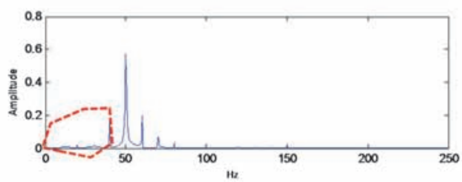

c) Order-2 intrinsic mode function (IMF2)

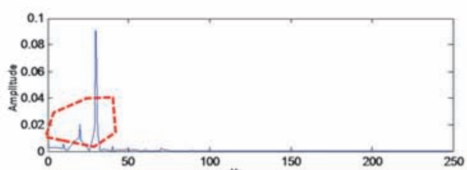

d) Order-3 intrinsic mode function (IMF3)

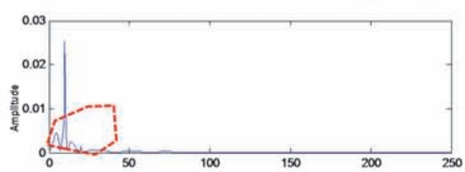

e) Order-4 intrinsic mode function (IMF4)

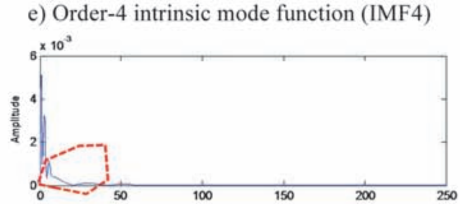

f) Order-5 intrinsic mode function (IMF5)

Fig. 2. The IMF components of the signal model obtained by the EMD.

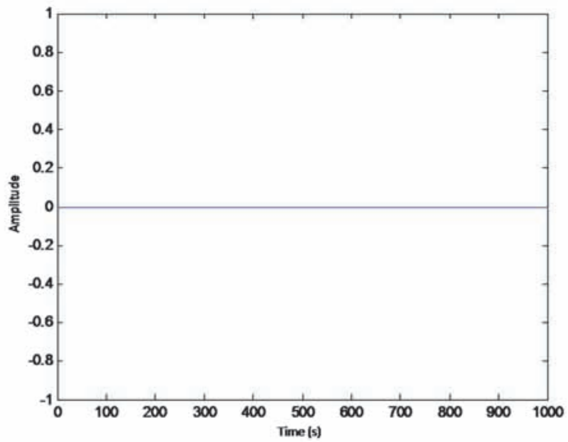

a) The residual error of LMD-based signal reconstruction

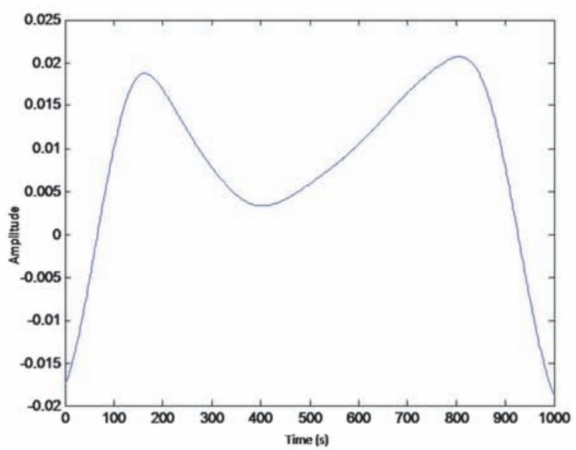

b) The residual error of EMD-based signal reconstruction

Fig. 3. The residual error of signal reconstructions.

SOBEL EDGE DETECTION AND COHERENCE

The Sobel algorithm is used in image processing and computer vision, particularly in edge detection. Technically, it is a discrete differentiation operator, computing an approximation of the greyscale of the image intensity function. At each point in the image, the result of the operator is either the corresponding grayscale vector or the norm of this vector (Kanopoulos et al., 2002). The Sobel algorithm is based on convolving the image with a small, separable, and integer-valued filter, that is, the coherence volume. The Sobel convolution factors are expressed below.

-1	0	1
-2	0	2
-1	0	1

a) G_x

1	2	1
0	0	0
-1	-2	-1

b) G_y

Fig. 4. The Sobel template of seismic edge detection. Note: G_x and G_y respectively represent image grayscales measured by horizontal and vertical edges.

The G_x and G_y can be calculated by the following equations:

$$G_x = \begin{bmatrix} -1 & 0 & +1 \\ -2 & 0 & +2 \\ -1 & 0 & +1 \end{bmatrix} * f(x,y) \quad , \tag{2}$$

$$G_y = \begin{bmatrix} -1 & +2 & +1 \\ 0 & 0 & 0 \\ -1 & -2 & -1 \end{bmatrix} * f(x,y) \quad , \tag{3}$$

where $f(x,y)$ is the grayscale of the seismic image; x and y are the coordinates of the location. The horizontal and vertical greyscales of each pixel in the image are combined to yield the size of the grayscale

$$G = \sqrt{G_x^{\ 2} + G_y^{\ 2}} \quad . \tag{4}$$

The greyscale G is considered as an edge if it surpasses a certain threshold. The Sobel algorithm can detect the extreme value at the edge, according to the upper and lower pixel points and the weighted different between left and right neighbours.

The background on the seismic data is mainly stratigraphic events. Coupled with seismic noise and faults, these events make it difficult to recognize the edges amidst the background and noise. Here, the seismic data are processed by the LMD filter to remove the noise. Then, the edges were calculated based on the coherence by Sobel algorithm, with the aim to discriminate faults from the background. The coherence was employed to characterize the discontinuity of the seismic data (Gersztenkorn and Marfurt, 1999; Kitchen and Rosenfeld, 2007). The coherence-based seismic edge detection can be expressed as:

$$G(t) = \sqrt{G_x^{\ 2} + G_y^{\ 2}} \quad , \tag{4}$$

where the $G(t)$ is the grayscale of the seismic image; t is the time. Thus, the 3D seismic data can be described as $f(x,y,t)$ with x and y being the horizontal and vertical axes of the volume, respectively.

SEISMIC DATA EDGE DETECTION AND FAULT MAPPING

Through the above description, the author developed a seismic edge detection method based on the local coherence of the detected edges. The method combines two important features of the seismic data: greyscale and discontinuity. Considering the high sensitivity to noise level, the LMD filter was introduced to remove the noise from the seismic data. After the filtering, the edges in the red circled zone (Fig. 5b) are much better delineated than those in that zone (Fig. 5a) of the original seismic data.

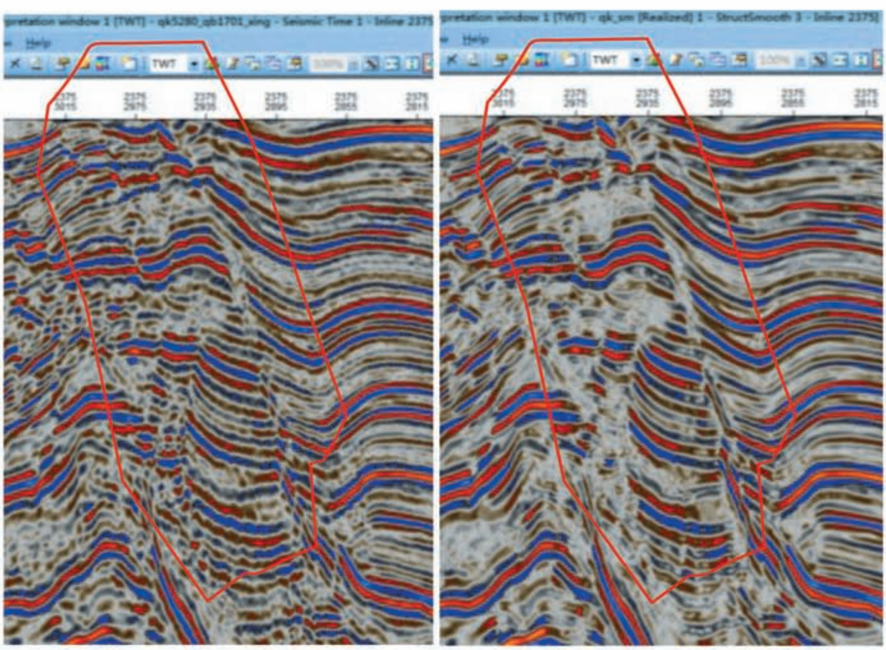

a) The original seismic data b) The filtered seismic data

Fig. 5. The seismic data (a) The red circled zone is the fault area in the original seismic data; b) The red circled zone contains the fault edges sharpened by the LMD filter.)

Then, the Sobel algorithm was adopted to compute an approximation of the greyscale of the image intensity function. The coherence (Fig. 6), as a priori knowledge on image type, was relied on to ensure the robustness of edge detection. On this basis, the edge localization properties were calculated, and the seismic discontinuities were transformed to similar greyscales.

As shown in Figs. 6a and 6b, the statistical properties of edge localization reveal that the noise is sensitive to coherence. According to the coherence-based edge detection results (Fig. 7), it is clear that the Sobel edge detection enhances the greyscale intensity and improves the mapping of discontinuous variation. Furthermore, the importance of the LMD filter to Sobel edge detection is demonstrated by the fewer stratigraphic events in Fig. 6b than Fig. 6a and in Fig. 7b than Fig. 7a.

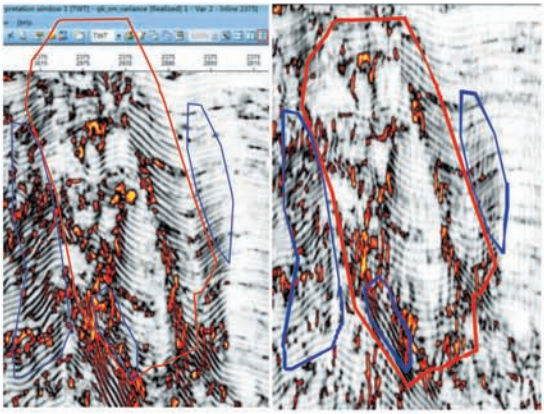

a) The original coherence b) The filtered coherence

Fig. 6. The coherence volume (a) The coherence calculated by the original seismic data, which contains stratigraphic events; b) The coherence calculated by the LMD filtered seismic data, which contains fewer stratigraphic events.)

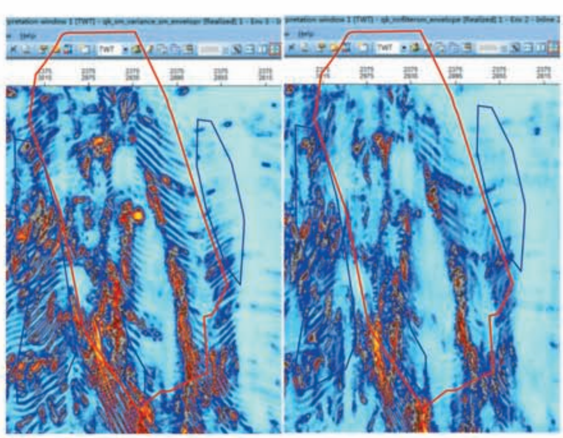

a) The original edge b) The filtered edge

Fig. 7. The edge volume (a) The edge volume calculated by the original coherence volume, which contains stratigraphic events in the blue circled area; b) The edge volume calculated by the coherence volume after LMD filtering, which contains fewer stratigraphic events.)

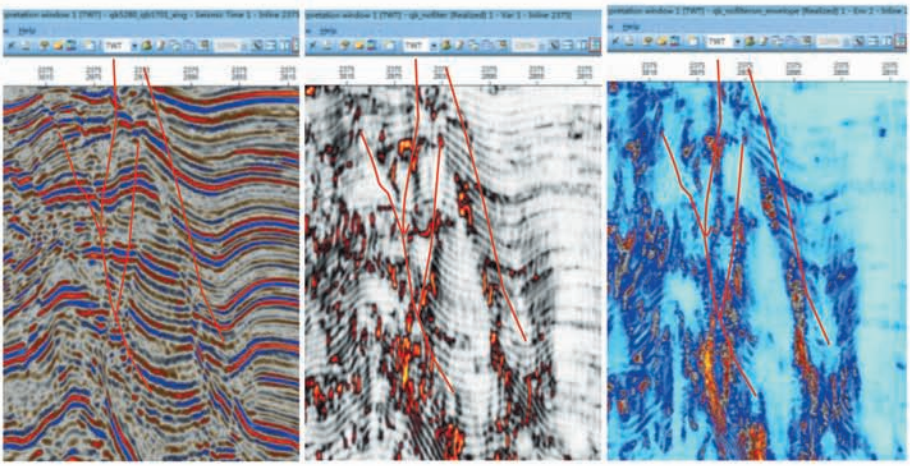

a) The seismic data b) The coherence volume c) The edge volume

Fig. 8. The seismic, coherence and edge volumes (a) The red lines represent the fault, which can be interpreted in the original seismic data. b) The red lines represent the fault, which can be interpreted in the coherence seismic data. c) The red lines represent the fault, which can be interpreted in the edge volume. And the edge volume where the fault can be obviously observed than b).

The points of sharp variation in edges and discontinuities are major indicators of faults in seismic data (Marfurt et al., 1998). In our research, the seismic edge detection results are used to map the seismic edges to seismic faults. The resultant seismic edges in Figs. 8b and 8c agree well with the faults in the original seismic data (Fig. 8a). Moreover, there are much fewer stratigraphic events in Fig. 8c than Fig. 8b. This means the Sobel edge detection method is applicable to the exploration and development of new fields.

CONCLUSIONS

This paper proposes a comprehensive method for seismic fault detection. Specifically, the seismic edge value was calculated based on coherence after LMD reconstruction. The PFs, subtracted from the original data, were used to reconstruct the signal and derive high-quality seismic data. The greyscales were computed by coherence, and taken as the priori knowledge to avoid the artificial edges on the seismic data. The results demonstrate that the seismic edges obtained by our method coincide with the seismic faults in the original seismic data, indicating that the proposed method can interpret the seismic edge data easily and rapidly. It is also verified that our method can detect the faults in the seismic data. This means the coherence-based method can detect unknown edges in the seismic data at a high accuracy.

ACKNOWLEDGMENTS

We thank the editor and the reviewer for their constructive comments and suggestions, which have helped to improve the quality of this paper. This study has been supported by the Scientific Research Projects of the Hubei Provincial Department of Education (B2017032; B2017029) and the PetroChina Innovation Foundation (2018D-5007-0301). This study has been funded by the Scientific Research Project of Yangtze University.

REFERENCES

Amstutz, S. and Fehrenbach, J., 2015. Edge detection using topological gradients: A scale-space approach. J. Mathemat. Imag. Vis., 52: 249-266. doi:10.1007/s10851-015-0558-z

Bahorich, M.S. and Farmer, S.L., 1995. 3D seismic discontinuity for faults and stratigraphic features: the coherence cube. The Leading Edge, 10: 1053-1058. doi:10.1306/64eda3e8-1724-11d7-8645000102c1865d

Cai, C., Ding, M.Y., Zhou, C.P. and Zhang T.X., 2004. Composite edge detector based on multi-wavelet operator. J. Image Graph., 9: 134-138. doi:10.11834/jig.20040222

Carter, N. and Lines, L., 2001. Fault imaging using edge detection and coherency measures on Hibernia 3-D seismic data. The Leading Edge, 20: 64-69. doi:10.1190/1.1438880

Chehrazi, A., Rahimpour-Bonab, H. and Rezaee, M.R., 2013. Seismic data conditioning and neural network-based attribute selection for enhanced fault detection. Petrol. Geosci., 19: 169-183. doi:10.1144/petgeo2011-001

Cohen, L., 1989. Time-frequency distributions-a review. Proc. IEEE, 77: 941-981. doi:10.1109/5.30749

Di, H. and Gao, D., 2014. Gray-level transformation and Canny edge detection for 3D seismic discontinuity enhancement. Comput. Geosci., 72: 192-200. doi:10.1190/segam2013-1175.1

Gersztenkorn, A. and Marfurt, K.J., 1999. Eigenstructure-based coherence computations as an aid to 3-D structural and stratigraphic mapping. Geophysics, 64: 1468-1479. doi:10.1190/1.1444651

Kanopoulos, N., Vasanthavada, N. and Baker, R.L., 2002. Design of an image edge detection filter using the Sobel operator. IEEE J. Solid-State Circ., 23: 358-367. doi:10.1109/4.996

Kitchen, L. and Rosenfeld, A., 2007. Edge evaluation using local edge coherence. IEEE Transact. Syst. Man Cybernet., 11: 597-605. doi:10.21236/ada109564

Krešić-Jurić, S., 2012. Analysis of edge detection in bar code symbols: An overview and open problems. J. Appl. Mathemat., 6: 1-16. doi:10.1155/2012/758657

Luo, Y., Higgs, W. and Kowalik, W., 1996. Edge detection and stratigraphic analysis using 3D seismic data. Expanded Abstr., 66th Ann. Internat. SEG Mtg., Denver: 324-331. doi:10.1190/1.1826632

Marfurt K.J., Kirlin, R.L., Farmer S.L. and Bahorich M.S., 1998. 3-D seismic attributes using a semblance-based coherency algorithm. Geophysics, 63: 1150-1165. doi:10.1190/1.1444415

Nadernejad, E., Sharifzadeh, S. and Hassanpour, H., 2008. Edge detection techniques: Evaluations and comparisons. Appl. Mathemat. Sci., 2: 1507-1520.

Park, C., Looney, D., Hulle, M.M.V. and Mandic, D.P., 2011. The complex local mean decomposition. Neurocomput., 74: 867-875. doi:10.1016/j.neucom.2010.07.030

Phillips, M. and Fomel, S., 2017. Plane-wave Sobel attribute for discontinuity enhancement in seismic images. Geophysics, 82: WB63-WB69. doi:10.1190/geo2017-0233.1

Rashmi, Kumar, M. and Saxena, R., 2013. Algorithm and technique on various edge detection: a survey. Sign. Image Process., 4: 65-75. doi:10.5121/sipij.2013.4306
Smith, J.S., 2005. The local mean decomposition and its application to EEG perception data. J. Roy. Soc. Interf., 2: 443-454. doi:10.1098/rsif.2005.0058
Wang, W., Gao J., Li K., Ma K. and Zhang X., 2009. Structure-oriented Gaussian filter for seismic detail preserving smoothing. IEEE Internat. Conf. Image Process., 601-604. doi:10.1109/icip.2009.5413869
Xu, H.Q. and Gui, Z.X., 2011. Progress of Edge Detection Technology in Seismic Exploration. Special Oil & Gas Reservoirs, 18: 7-10. doi:10.3969/j.issn.1006-6535.2011.04.002
Ziou, D. and Tabbone, S., 1998. Edge Detection Techniques-An Overview. Internat. J. Pattern Recognit. Image Analys., 8: 537-559.